Viscoelastic behavior of aqueous solutions of a polyoxyethylene-nonionic-amphiphile surfactant

G. D'Arrigo*
INFM, Dipartimento di Energetica, Università di Roma ''La Sapienza,'' Via Scarpa, 16-00161 Roma, Italy

G. Briganti
INFM, Dipartimento di Fisica, Università di Roma ''La Sapienza,'' Piazzale Aldo Moro, 2 00185 Roma, Italy
(Received 4 December 1997)

We present extensive measurements of shear viscosity, sound velocity, and ultrasonic absorption in aqueous solutions of the polyoxyethylene nonionic amphiphile $C_{12}H_{25}(OCH)_2(CH_2)_6OH$ (i.e., $C_{12}E_6$) in a wide temperature range (5–55 °C) and in a concentration range extending from the critical one up to the hexagonal mesomorphic phase. The static shear viscosity rapidly increases with concentration, and presents maxima as a function of temperature. The sound velocity exhibits an apparently complex behavior that can be interpreted as being due to a regular elastic contribution from the micellar moiety. Data on sound absorption in most concentrated solutions show unambiguous evidence of a viscoelastic behavior. Despite the qualitative similarity of our results with those observed in microemulsions of reversed micelles, the underlying interpretation is different. In particular, our analysis leads us to conclude that percolation phenomena due to increased connectivity cannot explain the sound velocity behavior. Rather, the sound velocity behavior can be related to the formation of long micellar structures which, on increasing temperature, become softer, likely resembling entangled polymeric solutions in a good solvent. [S1063-651X(98)01907-2]

PACS number(s): 62.60.+v, 82.60.Lf

I. INTRODUCTION

Viscoelasticity is not observed in ordinary molecular liquids of low viscosity. In such systems the static shear viscosity $\eta_{s,o}$ and the rigidity modulus G_∞ are of the order of 10^{-3} Pa s and 10^9 Pa, respectively, so that the characteristic (Maxwellian) time for the relaxation of the shear stresses ($\tau_s = \eta_{s,o}/G_\infty$) is about 10^{-12} s. Aqueous solutions of complex particles, depending on the temperature and on the concentration of the dispersed phase, present a wide variety of structural conformations and physical phenomena such as critical and percolation transitions, phase separation, and glass transitions. In these cases, an anomalous increase of $\eta_{s,o}$ and/or a rather low elastic modulus G_∞ may noticeably increase the relaxation time τ_s, giving rise to viscoelastic phenomena.

It is known that viscoelastic effects occur in supercooled liquids [1], in dilute polymer solutions [2], and in some concentrated micellar (e.g., bile salts) aqueous solutions [3]. Recently, they have also been observed in ternary supramolecular liquids consisting of oil, water, and surfactants forming microemulsions [4–7], as well as in concentrated $C_{10}E_5$ micellar solutions [8]. However, some of these observations [4,7,8] were based on the detection of a sound velocity dispersion rather than on the sound absorption behavior. As shown in Sec. II, this procedure cannot be considered probatory, but only indicative, and its analysis can lead to erroneous conclusions.

*Author to whom correspondence should be addressed: Giovanni D'Arrigo, Dipartimento di Energetica, Università ''La Sapienza,'' Via Scarpa 16, 00161 Roma, Italy. FAX: 39-6-44240183. Electronic address: darrigo@axrma.uniromal.it

The polyethylene nonionic amphiphiles $C_mH_{2m+1}(OCH_2CH_2)_nOH$ (briefly C_mE_n) have been extensively studied in wide surfactant concentration and temperature ranges [9]; there is evidence that up to ~50 wt % these systems maintain their micellar identity [8,10]. In the present paper, extensive density, viscosity, and ultrasonic (velocity and attenuation) measurements in $C_{12}E_6$ nonionic surfactant aqueous solutions are reported. The study of these properties directly verifies the occurrence of viscoelastic phenomena in complex binary systems and, in addition, should provide useful information about their structural and dynamical properties. Our results will be then compared with those found in other supramolecular liquids (e.g., microemulsions and polymers).

A partial view of the phase diagram of $C_{12}E_6$ binary solutions [11–13] is displayed in Fig. 1; the concentrations (in surfactant mass fraction percent w%) and temperatures investigated in our experiments are indicated as filled circles. Concerning the isotropic phase L_1, there are several experimental indications suggesting that this region is not morphologically uniform [12–15]. However, the structural changes of the micellar phase (size, shape, and growth) are rather controversial [14], but the view in the semidilute region is experimentally well defined. For example, electric birefringence studies [12] suggest that, as the surfactant concentration increases, the micellar shape changes from globular to long rodlike structures. These structures, near the border of the H_1 phase, are partially aligned, a precursive condition of the adjacent hexagonal liquid crystal phase. At higher temperatures these experiments indicate the occurrence of a shape transition toward disklike micelles, precursive of the lamellar phase L_α, present at the same temperature but at higher concentrations. Similarly, light scattering experiments [15] suggest that semidilute solutions at high temperature

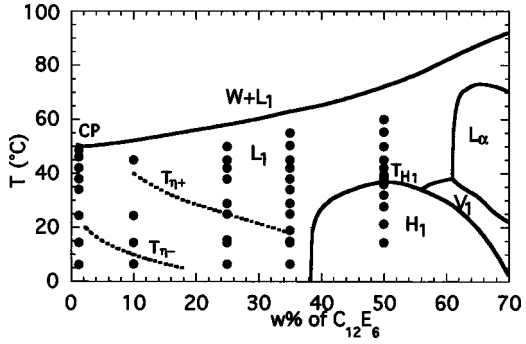

FIG. 1. A limited temperature concentration (wt %: mass fraction percent of surfactant) portion of the phase diagram of the water-$C_{12}E_6$ system. L_1: isotropic micellar phase; $W-L_1$: two phases region delimited by the coexistence line; CP: critical point; H_1: hexagonal crystalline phase; T_{H_1}: higher melting temperature of the H_1 phase; L_α: lamellar phase; T_{η^-}: line of viscosity minima in the plot of Fig. 2; T_{η^+}: line of viscosity maxima in the plot of Fig. 2; the filled circles indicate the samples investigated in the present ultrasonic measurements.

resemble entangled solutions of flexible polymers that, at higher concentrations, transform into regions of rodlike and disc structures. Other studies indicate transitions toward aggregation of small micelles, random percolating clusters or liquid crystalline clusters [16]. In any case, the rich variety of structural conformations present in the phase diagram of $C_{12}E_6$ make these solutions very appropriate for a detailed analysis of viscoelastic properties.

Current theoretical models for micellar formation can predict a temperature evolution of micellar shape, but very few theoretical predictions are available for the concentration dependence of micellar distribution function [17]. Recent models developed for liquid systems formed by assembly of hard spheres having a weak interparticle attraction suggest, at higher concentrations, a tendency toward the formation of extended structures [18].

In Sec. II, we summarize the theoretical background on sound propagation in viscoelastic media used in our ultrasonic data analysis. After the experimental section (Sec. III), in Sec. IV we present and analyze the experimental results. Discussions and conclusions are given in Secs. V and VI.

II. SOUND PROPAGATION IN VISCOELASTIC MEDIA

The response of a viscoelastic medium to an alternating pure shear stress can be characterized by a complex rigidity modulus $\mathbf{G}(\omega)$ or by a complex shear viscosity $\boldsymbol{\eta}_s=\mathbf{G}/\mathbf{i}\omega$. Similarly, a complex bulk modulus $\mathbf{K}_r(\omega)$ or a complex bulk viscosity $\boldsymbol{\eta}_b=\mathbf{K}_r/\mathbf{i}\omega$ characterizes the response to a pure compressional stress. An ultrasonic longitudinal wave of frequency $\omega(=2\pi f)$ propagating in a medium contains both components and the propagation involves both moduli and viscosities. Considering a longitudinal complex modulus $\mathbf{M}(\omega)=\mathbf{K}(\omega)+\frac{4}{3}\mathbf{G}(\omega)$, in the limits $\alpha\lambda\ll 4\pi^2$, we have the results [1,2]

$$c^2(\omega)\cong\frac{M'(\omega)}{\rho} \tag{1}$$

and

$$\alpha\lambda\cong\pi\frac{M''(\omega)}{M'(\omega)}. \tag{2}$$

Equations (1) and (2) relate the moduli to the measured sound velocity (c) and to the attenuation coefficient (α) per wavelength (λ). In addition, there are

$$\mathbf{K}=K'+\mathbf{i}K''=[K_0+K_r'(\omega)]+\mathbf{i}K_r''(\omega)=\rho c_0^2+\mathbf{i}\omega\boldsymbol{\eta}_b(\omega) \tag{3}$$

and

$$\mathbf{G}=G'+\mathbf{i}G''=\mathbf{i}\omega\boldsymbol{\eta}_s(\omega). \tag{4}$$

One can also define a longitudinal complex kinematic viscosity ($\mathbf{D}_1$) given by $\mathbf{D}_1=\rho^{-1}[\boldsymbol{\eta}_b(\omega)+\frac{4}{3}\boldsymbol{\eta}_s(\omega)]$, so that $\mathbf{M}=\rho[c_0^2+\mathbf{i}\omega\mathbf{D}_1(\omega)]$. Equations (1) and (2) can be then put in the forms

$$c^2(\omega)=\rho^{-1}[K_0+K_r'(\omega)+\tfrac{4}{3}G'(\omega)] \tag{1'}$$

and

$$\alpha\lambda=(\pi\omega/\rho c^2)[K_r''(\omega)/\omega+\tfrac{4}{3}G''(\omega)/\omega], \tag{2'}$$

or, equivalently,

$$\alpha/f^2=(2\pi^2/\rho c^3)[\eta_b(\omega)+\tfrac{4}{3}\eta_s(\omega)] \tag{5}$$

The frequency dependencies of c and α/f^2 are related to the peculiar dynamics of the bulk and shear viscosity. For a Debye (single time) relaxation, this is

$$K_r'(\omega)=K_r[\omega^2\tau_b^2/(1+\omega^2\tau_b^2)],$$

$$K_r''(\omega)=\omega\eta_b(\omega)=K_r[\omega\tau_b/(1+\omega^2\tau_b^2)],$$

and

$$G'(\omega)=G_\infty[\omega^2\tau_s^2/(1+\omega^2\tau_s^2)],$$

$$G''(\omega)=\omega\eta_s(\omega)=G_\infty[\omega\tau_s/(1+\omega^2\tau_s^2)],$$

where τ_b and τ_s are the relaxation times for compressional and shear processes, respectively. In the limits $\omega\tau_b\ll 1$ and $\omega\tau_s\ll 1$ (low frequencies), one obtains

$$c^2(\omega)\approx c_0^2=K_0/\rho,\quad (\alpha/f^2)_0=(2\pi^2/\rho c_0^3)[\eta_{b,0}+4/3\,\eta_{s,o}]. \tag{6}$$

(i.e., c and α/f^2 are independent of frequency) where $\eta_{b,0}=K_r\tau_b$ and $\eta_{s,o}=G_\infty\tau_s$ are the static bulk and shear viscosity, respectively.

In the limits $\omega\tau_b\gg 1$ and $\omega\tau_s\gg 1$ (high frequencies), the dynamics is

$$c_\infty^2(\omega)=c_0^2+\rho^{-1}(K_r+4/3G_\infty),\quad (\alpha/f^2)_\infty\to 0.$$

In the case of continuous distributions of relaxation times (e.g., Cole-Cole, Cole-Davidson, Havriliah-Negami, and Watt-Williamson) appropriate expressions for $\mathbf{K}(\omega)$ and $\mathbf{G}(\omega)$ must be used.

In ordinary molecular fluids of low shear viscosity, where typically $\eta_{s,o}\approx 10^{-3}$ Pa s, $G_\infty\approx 10^9$ Pa, and $\tau_s\approx 10^{-12}$ s, normally $\omega\tau_s\ll 1$ and $\omega\tau_b\approx 1$, so that

$$c^2(\omega)=c_0^2+\rho^{-1}[K_r(\omega)+4/3G_\infty]$$

and

$$\alpha/f^2=(2\pi^2/\rho c^3)[\eta_b(\omega)+4/3\eta_{s,o}]=(\alpha/f^2)_{\rm bulk}+(\alpha/f^2)_{\rm NS}.$$

In such systems one often observes sound velocity dispersion and a frequency dependent α/f^2, which are due to the first term in the previous equation, i.e., the relaxation behavior of the bulk viscosity (e.g., structural, chemical, conformational or other processes). But in ordinary liquids the experimental α/f^2 is never lower than the so-called Navier-Stokes (NS) contribution $(\alpha/f^2)_{\rm NS}=(8\pi^2/c^3)(\eta_{s,o}/\rho)$ due to the steady shear viscosity.

In viscoelastic media where the relaxation time τ_s can be comparable to the characteristic ultrasonic times ($\omega^{-1}\approx 10^{-6}-10^{-9}$ s), one can observe the relaxation behavior of both bulk and shear viscosity. In such media, however, independent measurements of the dynamic shear viscosity $\eta_s(\omega)$ are necessary to disentangle the two contributions. In any case, experimental α/f^2 values lower than $(\alpha/f^2)_{\rm NS}$ represent direct evidence of viscoelastic effects.

III. EXPERIMENTAL METHODS

Measurements were mainly performed along isoconcentred paths in the homogeneous isotropic region L_1 above CMC. However, one of these paths (50 wt %) crosses the hexagonal liquid crystal phase H_1 at its melting temperature $T_{H_1}=37$ °C. Measurements realized with different techniques were performed at about the same temperature and concentration ranges. When needed in the analysis, interpolated data were used.

A. Samples

The $C_{12}E_6$ (purity≈99%; M.W.=450.66; m.p. 27–28 °C) was purchased from Nikko Chemical and used without further purification. The sample solutions used in the density, viscosity, and ultrasonic experiments were prepared just before the beginning of each measurement, the compositions being determined by weighting. The studied concentrations ranged from about 1–50 wt %. The investigated temperature interval varied from about 5 °C to the corresponding cloud temperatures where the samples separate.

The CMC of $C_{12}E_6$ solutions was given by Balmbra *et al.* [19] as $c_o=8.7\times10^{-5}$ M at 25 °C corresponding to ≈0.004 wt %. Critical parameters of the system [20,21] are $w_{\rm crit}=1.25$ wt % and $T_{\rm crit}=50.2$ °C. All the investigated samples are therefore well above the CMC, one of them having the critical concentration.

B. Density

The densities of solutions (ρ), needed in the analysis, were measured with a vibrating tube densimeter (PAAR model DMA 602) having six decimal digits for density determinations (PAAR DMA60); the apparatus was calibrated using water and air as references at all the temperatures used in the experiments. Detailed results and discussion of the density data are reported elsewhere.

The volume fraction (ϕ) of the dispersed phase (surfactant) was evaluated, as usual, from the density data using the relation $\phi=1-(1-w)\rho/\rho_w$, where ρ_w is the water density and w(=wt %/100) the mass fraction of the surfactant. For practical purposes, since $\rho\approx\rho_w$, $\phi\approx w$.

C. Shear viscosity

Kinematic shear viscosity measurements at various concentrations as a function of temperature were performed with standard calibrated Ubbelhode tubes. Using viscometers with different constant ($100-500\ s^{-1}$) we found nearly equivalent values, indicating that in such a range the measured viscosity represents the static (zero-frequency) values. The steady shear viscosity of solutions ($\eta_{s,o}$) is obtained from the kinematic data multiplying by the density. The viscosity of solutions relative to water, $\eta_r=\eta_{s,o}/\eta_w$, was calculated using for $\eta_w(t)$ the approximated expression $\eta_w(mP)=3.271+14.261\exp(-0.036\,97\,t)$.

D. Ultrasounds

A variable path-length cell was used for the ultrasonic measurements. The cell content was about 30 ml of solution. Two matched 5-MHz fundamental crystals were used, along with a quartz delay line, in a pulsed-sound mode. The temperature of the sample was controlled by a water thermostat regulated within ±0.1 K.

Sound attenuation was measured [22] by a standard pulse technique using Matec equipment. The sound absorption coefficient (α) in the range from 5 to about 155 MHz was obtained measuring the amplitude loss of the first pulse traversing the sample (before any reflections) and was accurate within 5%.

The sound velocity (c) was obtained by acoustically overlapping pulses under variable, path conditions to coherent cw signals generated by a Matec Pulse Modulator equipment [22]. Among various techniques tried, the one used was found to be the most reliable for detecting sound velocity dispersion within ±1 m s in the frequency range 5–75 MHz. However, in highly attenuating samples, its application reduces up to about 50 MHz. As a consequence, measurements were performed, as a rule, at 5 and 45 MHz. In some cases they covered all the intermediate allowable frequencies (15, 25, and 35 MHz). The accuracy of the absolute sound velocity data (at fixed frequency) is estimated to be ±0.2 m/s over the whole frequency range.

IV. RESULTS AND ANALYSIS

A. Viscosity

In Fig. 2, we display the relative viscosity of the studied solutions (0–25 wt %) as a function of temperature. Also shown in the figure are some data from Ref. [12] which extend to 35 wt %. As can be seen, a substantial agreement exists among the two sets of data.

Characteristic features of this figure are the large increase of viscosity with increasing concentration, and its temperature dependence. In particular, in the concentration region 0–18 wt % η_r is independent of temperature up to a value

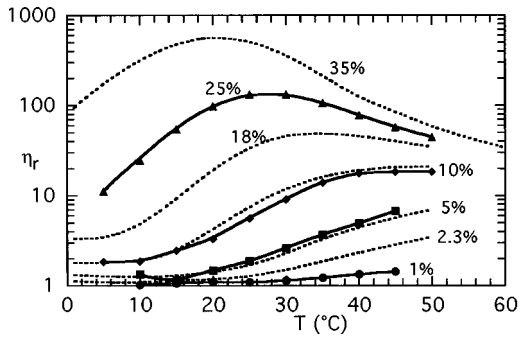

FIG. 2. Relative viscosity $\eta_r = \eta_{s,o}/\eta_{\text{water}}$ of solutions as a function of temperature for different volume fractions ϕ of the surfactant. Symbols and continuous lines: our measurements. Dotted lines: data from Ref. [13]. Lines are smooth curves through the experimental data. Note the presence of concentration-dependent flat trends and maxima of viscosity. The corresponding temperatures ($T_{\eta-}$ and $T_{\eta+}$) are displayed in Fig. 1.

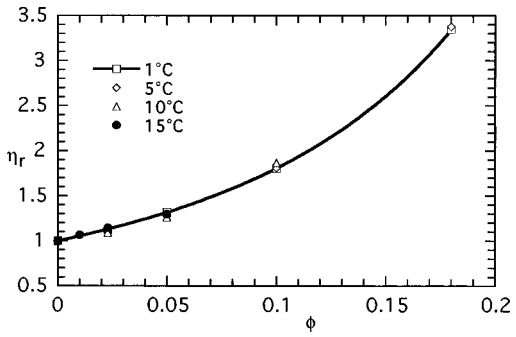

FIG. 3. Relative viscosity η_r vs the volume fraction ϕ of the solutions located below the $T_{\eta-}$ line in Fig. 1. All data are well fitted by a single curve (continuous line) representing Eq. (9).

$T_{\eta-}$, which decreases with increasing concentration. For higher concentrations, η_r increases with temperature up to a maximum at a temperature $T_{\eta+}$, which also decreases as the concentration increases. Plots of the concentration dependence of both $T_{\eta-}$ and $T_{\eta+}$ are displayed in Fig. 1 as dotted lines. In solutions lying below the $T_{\eta-}$ line in Fig. 1, the relative viscosity is then roughly independent of temperature.

We point out that the viscosity data at 1.25 wt % (the critical concentration) do not exhibit the typical divergence of critical mixtures. However, our data extend to about 5 °C below the critical temperature (50.2 °C), and critical effects in the viscosity are usually seen 1 K far from the critical temperature T_c [23].

Viscosity maxima similar to those in Fig. 2 have also been found in $C_{14}E_8$ aqueous solutions [16], but not in C_8E_5 solutions [24]. In the first system, however, the phase diagram is similar to that in Fig. 1, while in C_8E_5 solutions the lyotropic phases are absent. This suggests that the existence of viscosity maxima could be related to the presence of ordered phases.

A viscosity behavior such as that in Fig. 2 is also found in microemulsions [23,25,26]. In such systems the large enhancement of η_r is related to a percolationlike transition which, in turn, is based on aggregation or polymeric growths processes originated by attractive interactions [27].

We first analyzed our viscosity data according to the current models for colloidal systems. In the dilute limit, if hard, noninteracting particles are present, the relative viscosity should increase with ϕ according to the hydrodynamic Stokes-Einstein expression $\eta_r = 1 + k\phi$, where k is a constant characteristic of the particle geometry ($k = \frac{5}{2}$ for a sphere, and larger for asymmetric shapes). The equation is considered valid up to $\approx \phi = 0.02$. At larger concentrations, packing effects and interactions modify the Einstein equation, and several phenomenological expressions have been proposed. Among these we quote the virial-type one [23]

$$\eta_r = 1 + k_1\phi + k_2\phi^2 + k_3\phi^3 + \cdots, \tag{7}$$

where k_i are constants and $k_1 = k$, and the Mooney expression [28]

$$\eta_r = \exp[k\phi/(1 - m\phi)], \tag{8}$$

where m is an interaction parameter. In the dilute limit both equations reduce to the Einstein expression. A more physical relation, which explicitly takes into account packing effects and repulsive interactions between nonaggregated particles in diluted solutions, has been recently used in microemulsions [25]. This expression,

$$\eta_r = (1 + k\phi) + A\{(\phi/\phi_m)^{(n+1)/3}[1 - (\phi/\phi_m)^{1/3}]^{-n}\}, \tag{9}$$

contains an hydrodynamic term superimposed on an interaction contribution related to the random close-packing volume fraction (ϕ_m), and to the exponent (n) of the repulsive part of the potential.

If aggregation does not occur, the parameters in Eqs. (7)–(9) are temperature independent. When particles aggregate and/or attractive contributions play a relevant role, the parameters in the previous equations depend on the temperature or take unphysical values.

In Fig. 3, we plot the ϕ dependence of the viscosity of the solutions in the low (ϕ,T) range (about $0 < \phi < 0.18$; $1 < T < 15$ °C) below the $T_{\eta-}$ line. Any one of Eqs. (7)–(9) fit well the experimental data with temperature independent parameters.

In Fig. 4, we plot the overall viscosity data as a function of volume fraction. We find that for temperatures up to 15–20 °C the data can still be fitted by Eqs. (7)–(9) over the entire concentration range, but in such fittings the parameters change with temperature. Fits with Eq. (8) for $T = 1$, 5, 10, and 15 °C are shown in Fig. 4 by solid lines. For temperatures equal to and above 20 °C, the data cannot be fitted by any of Eqs. (7)–(9) since the parameters assume unphysical values. The dotted lines in Fig. 4 are only to guide the eyes through such data.

From a viscosity analysis, we have some indications that below the $T_{\eta-}$ line the solute structure is well represented by small spheroidal and repulsive particles, since the parameters in the viscosity equations (7)–(9) are independent of temperature. By contrast, the large viscosity and its dependence on the temperature above the $T_{\eta-}$ line indicates the presence of solute-solute attractive interactions and/or self assembling.

From our analysis, we are not able to assign a physical meaning to the $T_{\eta+}$ curve in Fig. 1. Looking at the qualitative analogy with the viscosity behavior in microemulsions,

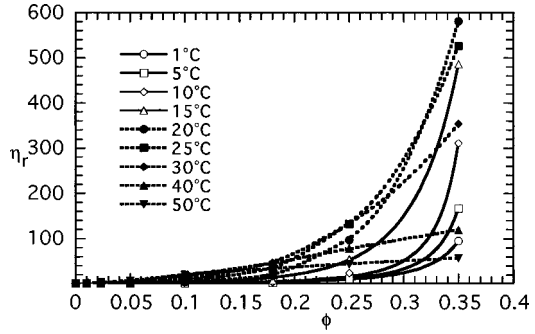

FIG. 4. Overall relative viscosity data as a function of volume fraction for some interpolated temperatures. For temperatures below 20 °C, the data can still be fitted approximately by Eqs. (7)–(9) (solid lines) with temperature-dependent free parameters. For higher temperatures the data can no longer be fitted by Eqs. (7)–(9) and/or free parameters assume unphysical values. Dotted lines are guides to the eyes for these high-T data. They roughly correspond to solutions lying above the T_{η_-} line in Fig. 1.

one is tempted to link this line to a percolationlike behavior. However, such a connection seems to be excluded by the analysis of the sound velocity in Sec. V.

B. Sound velocity

The experimental sound velocity behaviors as a function of temperature and concentration are shown in Figs. 5(a) and 5(b). Data for pure water are in good agreement with those reported in literature [29], those for pure liquid $C_{12}E_6$ were taken from Ref. [30] (5 MHz, range 20–45 °C).

Data in the figures refer to 5 MHz. No appreciable sound velocity change with the frequency was detected in the range 5–45 MHz for all the investigated concentrations and temperatures. Despite this finding, the measured sound velocities (and the related quantities) must be considered as dynamic and, thus, in principle, different from the static (thermodynamic) values. We come back to such an aspect in the analysis of the sound absorption.

The temperature dependence in the figure shows that, as the amount of surfactant increases, the sound velocity behavior in the solutions gradually shifts from that characteristic of water (i.e., positive temperature coefficient) to that characteristic of a pure surfactant (i.e., negative coefficient). However, at low temperatures, the sound velocity is larger than in water, thereafter becoming lower with a crossing region at about $T^* \approx 34$ °C.

We must also note that the curves in Fig. 5(a) are rather smooth for all concentrations. However, a detailed inspection of the sound velocity curve at 50 wt % shows a small change in the slope at ~ 38 °C. This temperature, indicated by an arrow in Fig. 5(a), corresponds to the upper limit ($T_{H_1} \approx 37$ °C) of the middle phase region reported in Fig. 1.

The qualitative behaviors of the sound velocity as a function of both temperature and concentration in Figs. 5(a) and 5(b) are quite different from those found in microemulsions forming reversed micelles [4–7]. However, this finding is not surprising, since in our system the embedding medium is water, while in microemulsions it is oil. The following analysis will take into account this observation.

As shown in Sec. II, the sound velocity is related to the real part M' of the longitudinal modulus. In order to analyze our velocity data, it is also useful to consider the adiabatic compressibility $\beta[=V^{-1}(\partial V/\partial p)_S]$, which is the inverse of M', i.e., $\beta=(M')^{-1}=(\rho c^2)^{-1}$.

We previously noted that as the concentration of surfactant increases, the sound velocity as a function of temperature gradually shifts from that characteristic of water to that characteristic of a surfactant. Qualitatively this trend is expected in ideal solutions where, due to the absence of interactions, volume and internal energy are additive. Accordingly, the ideal isoentropic compressibility ($\beta_{\rm id}$) of solutions is approximately given by $\beta_{\rm id}=(1-\phi)\beta_w+\phi\beta_s$, i.e., it is a volume-weighted mix of the compressibility β_w and β_s of pure components. The previous relation is rigorously valid in the limit $\omega \to 0$ and under isothermal conditions. In fact, due to the entropy of mixing, small corrections should be added to the previous expression [31]. The sound velocity of an ideal solution is given by $c_{\rm id}=(\rho_{\rm id}\beta_{\rm id})^{-1/2}$, and that of the ideal real modulus ($M'_{\rm id}$) by

$$\frac{1}{M'_{\rm id}}=\frac{(1-\phi)}{M'_w}+\frac{\phi}{M'_s}, \tag{10}$$

and it can be evaluated by means of the densities and sound velocities in pure components.

Comparing the experimental $M'=\rho c^2$ and the ideal $M'_{\rm id}$ moduli, we find differences that demonstrate the nonideality of the system. In Figs. 6(a) and 6(b), we plot this excess modulus $\Delta M'=M'-M'_{\rm id}$ as a function of temperature and concentration. $\Delta M'$ can be considered representative of the departure of the system from ideality, and then of the inter-

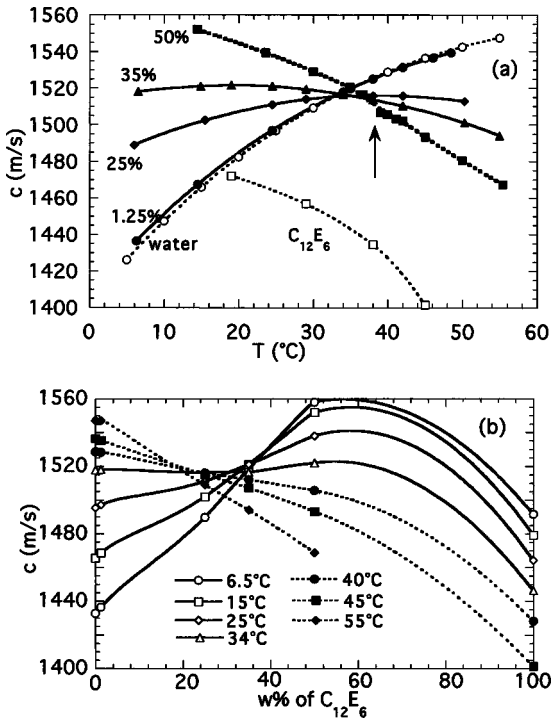

FIG. 5. The temperature (a) and concentration (b) dependence of the ultrasonic velocity at 5 MHz. Lines are guides to the eyes. In the overall solutions no appreciable sound velocity dispersion was detected in the investigated frequency range 5–55 MHz. The arrow in the sample 50 wt % in (a) indicates the temperature ($\approx T_{H_1}$), where the sound velocity exhibits a small discontinuity.

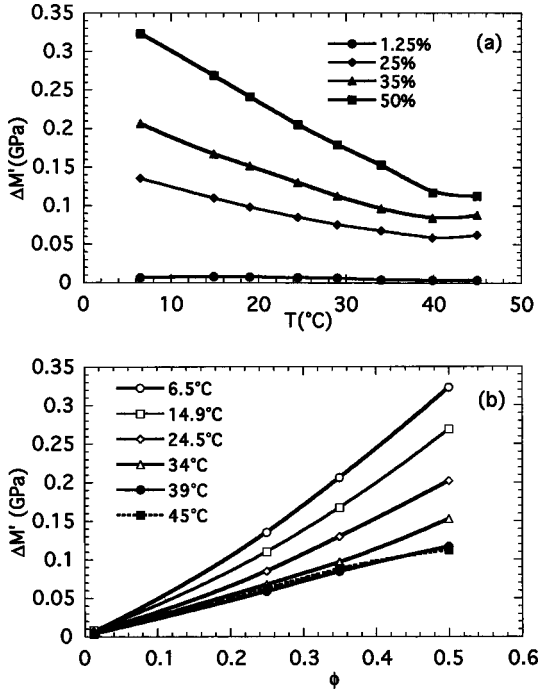

FIG. 6. The ''excess'' real longitudinal modulus $\Delta M' = M' - M'_{\mathrm{id}}$ as a function of temperature (a) and concentration (b). M' is the experimental ultrasonic value ($=\rho c^2$), and M'_{id} is calculated from a volume-weighted mix of the compressibility of the constituent components [Eq. (10)]. $\Delta M'$ can be considered representative of the departure of the system from ideality, and of interactions in the system.

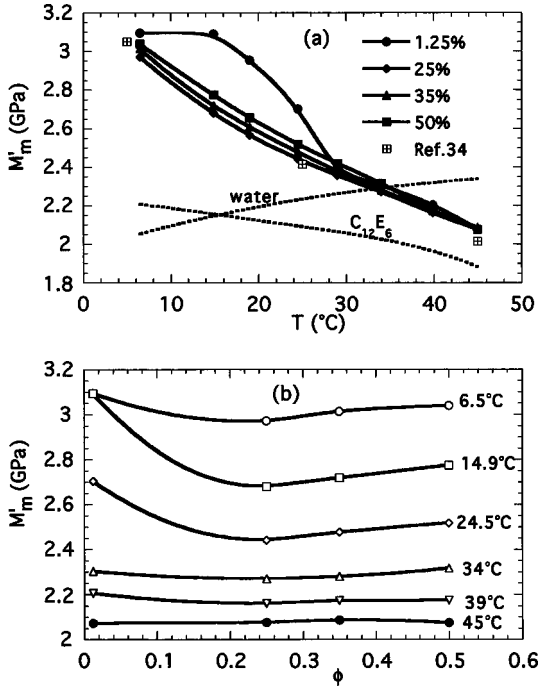

FIG. 7. The temperature (a) and concentration (b) dependence of the micellar real longitudinal modulus M'_m. M'_m is calculated from the moduli of solutions and of the water by using the effective-medium relation [Eq. (11)].

actions in the system. Such an approach was discussed in a previous paper [32], where a similar quantity ($c^2 - c_{\mathrm{id}}^2$) was used to obtain exponents of the attractive and repulsive terms in the interaction potential. From a phenomenological point of view, we can take into account departure from ideality by considering an asymmetric solution where one component is unperturbed water molecules, and the other one surfactant molecules engaged in a micellar phase; this phase possesses its own, unknown, elastic properties similar to but different from those of pure liquid $C_{12}E_6$. This picture is also suggested by currently accepted models for nonionic micelle aggregation, according to which the solute-solvent interactions are mainly restricted to the oxyethylene groups of the surfactant molecules in the micelles (heads) and few hydration water molecules. Accordingly, we write the volume (V) of a solution of m_w grams of water and m_s grams of surfactant as $V = m_w V_{w+} m_s V_m$, where V_w and V_m are, respectively, the specific volumes of bulk water and surfactant in micellar conditions. Deviation from ideality is then taken into account by assuming $V_m \neq V_s$, the volume of the pure surfactant. On writing the previous expression for V we neglected contributions from surfactant monomers, since our concentrations are well above the CMC.

As for β_{id}, we can write the compressibility of solutions as $\beta = (1-\phi)\beta_w + \phi\beta_m$ or, in terms of moduli,

$$\frac{1}{M'_{\mathrm{id}}} = \frac{(1-\phi)}{M'_w} + \frac{\phi}{M'_m}. \tag{11}$$

This relation is also known as the Wood's effective-medium relation, and it was extensively used in microemulsions [4–7] and other amphiphilic aqueous solutions [8,33]. Although Eq. (11) is strictly valid in the static limit $\omega \to 0$, we will use it to find the real modulus of the micellar phase M'_m at the investigated frequencies.

Likewise, $\Delta M'$, M'_m should express the departure of solutions from ideality and, in particular, represent the elasticity of the micellar aggregates in the solutions. The T and ϕ dependencies of M'_m, evaluated by means of Eq. (11), are displayed in Figs. 7(a) and 7(b), respectively. For comparison, we also show in the figure the values obtained in Ref. [34] from measurements in diluted solutions at 5, 25, and 45 °C. In the low concentration range investigated by these authors (up to $\phi = 0.015$), M'_m resulted independently of concentration. In the figure we also display the moduli in the pure components (in their bulk liquid state).

Looking at the behaviors in Fig. 7, we can distinguish two regions. Concentrated solutions ($\phi \geqslant 0.25$) exhibit micellar moduli that depend slightly on concentration, and decrease rapidly and smoothly with temperature. In contrast, in dilute solutions (our $\phi = 0.0125$ and $0.0004 < \phi < 0.015$ from data in Ref. [34], M'_m is temperature independent at low temperatures ($\approx T < 15$ °C), thereafter decreasing with temperature like in concentrated solutions. Then the overall behaviors indicate the following. (a) The micellar structure in the low (ϕ, T) region is harder than that in the highest range. Again, this observation agrees with the conjecture (suggested by the viscosity analysis) that the morphological structure of solutions below and above the line $T_{\eta-}$ in Fig. 1 is different. (b) There exist a substantial continuity in the elastic properties of the micellar phase in the region above $T_{\eta-}$; in particular, there are no peculiar trends or changes on crossing the line $T_{\eta+}$. (c) The smooth changes of M'_m above $T_{\eta-}$ depend

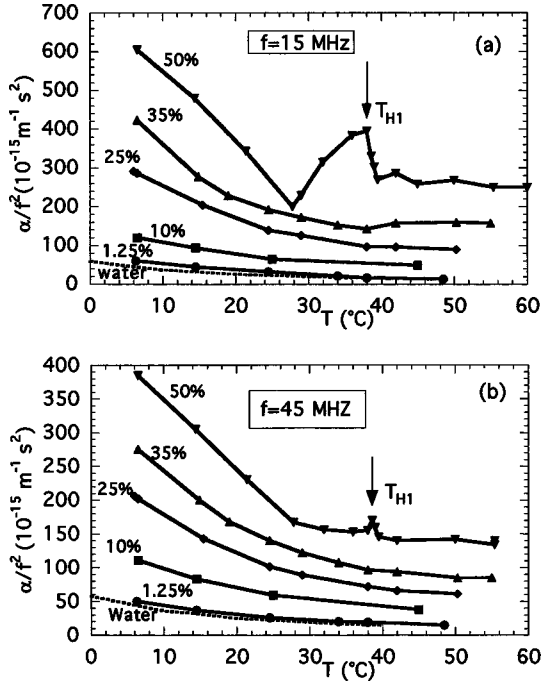

FIG. 8. Ultrasonic attenuation (α/f^2) as a function of temperature at the investigated concentrations: (a) 15 MHz; (b) 45 MHz. Lines are only guides to the eyes.

mainly on T rather than ϕ, the micellar structure becoming softer and softer with an increase of temperature.

C. Ultrasonic attenuation

The dependences of the ultrasonic attenuation (as expressed by the usual α/f^2 plot) on the temperature in the investigated concentrations at 15 and 45 MHz are shown in Figs. 8(a) and 8(b), respectively. We can note that, in general, attenuation increases with increasing concentration and decreases as T increases.

In the sample $\phi=0.5$, the crossing of the phase boundary at T_{H_1} is evident. Starting from ~ 15 °C and increasing the temperature, the attenuation decreases rapidly. However, from ~ 30 to 38 °C, the system seems to become unstable, as suggested by the dispersion of the sound attenuation values obtained from different measurements. Data points displayed in the figures are average values over several runs performed at each temperature. The sharp increase of α/f^2 at temperatures close to 38 °C is, however, well established. Similar behaviors have been observed in other concentrated micellar solutions [35–37]. Ultrasound studies [38] near the lyotropic-isotropic transition in liquid crystals have found critical fluctuation contributions to the sound absorption on both sides of the transition. The anomalous attenuation we find at T_{H_1} is then likely related to critical effects.

We also observe that the decreasing trend with temperature is found in the sample of critical concentration (1.25 wt %) on approaching the critical point. Although the studied temperature interval was not extended very near to the critical point, the results clearly indicate an apparent lack of a sound absorption critical anomaly (divergentlike behavior) for temperatures up to 5 °C of T_c. This trend, which is in contrast to that observed in molecular binary solutions, has already been noticed in several supramolecular critical systems [33,39,40]. However, recent experiments [41,42] showed that the absorption critical anomaly in supramolecular liquids extends in a very narrow T range around T_c.

Figure 8 shows that α/f^2 values at 45 MHz are lower than at 15 MHz. In order to investigate the relaxation behavior in detail, we performed measurements in the range 5–155 MHz in the samples of 1.25, 10, 25, 35 and 50 wt % at some temperatures.

At 1.25 wt % and for each temperature the ultrasonic absorption resulted to be low (slightly higher than in water) and weakly dependent on the frequency. As a consequence, it cannot be used for a reliable analysis of the spectra. However, α/f^2's values at the highest frequencies resulted to be higher than the Navier-Stokes contribution $(\alpha/f^2)_{\mathrm{NS}}=(2\pi^2/\rho c^3)\eta_{s,o}$ calculated from sound velocity and kinematics viscosity $\eta_{s,o}/\rho$ data, using either the solvent or the solution viscosity. This finding led us to exclude the occurrence of viscoelastic effects in these solutions. Detailed ultrasonic studies in several diluted C_nE_m solutions [43] confirm this observation, attributing the observed excess absorption to bulk viscosity processes related to the perturbation of some chemical equilibria between the micelles and the surrounding medium (surfactant monomers and/or water molecules). The Aniansson-Wall [44] and Teubner [45] theories account for the T and concentration behaviors of such effects. Characteristic rates of these equilibria (relaxation frequencies) are on the order of 0.1–5 MHz.

In Figures 9(a), 9(b), 9(c), and 9(d), we report the relaxation spectra of the samples at concentrations $\phi=0.1$, 0.25, 0.35, and 0.50 at various temperatures in the isotropic region. The lines are the results of a fitting procedure discussed below. The relevant finding in these spectra is that most of them exhibit a viscoelastic behavior since $(\alpha/f^2)_{\mathrm{exp}}<(\alpha/f^2)_{\mathrm{NS}}$. However, in the sample of $\phi=0.1$ at $T=6.5$ and 14.5 °C, located below the T_{η^-} curve in Fig. 1, the effect is not found.

The measured ultrasonic spectra were fitted to several known relaxation expressions, which, in general, can be written in the form

$$\alpha/f^2=AF(f^*,a,b)+B_\infty, \tag{12}$$

where A is an amplitude, $f^*=\omega\tau=f/f_r$ is a reduced frequency (τ is the relaxation time, and f_r the relaxation frequency), a,b are free parameters, and B_∞ is a background contribution from relaxation processes occurring at frequencies well above the highest f of the measurements. For discrete distributions it is $F(f^*)=[1+(f/f_r)^2]^{-1}$ (single relaxation), or a sum of two of such equations for a double relaxation. For continuous distributions, $F(f^*,a,b)$ takes appropriate expressions. In our fit we considered the Havriliak-Negami, Cole-Cole, Cole-Davidson, and Romanov-Solovyev distributions containing parameters (such as a,b) describing the shape and width of the distribution. We also used the fitting equation $\alpha/f^2=Af^{-n}+B_\infty$ ($n=\frac{1}{2}$ or $\frac{1}{3}$) describing the Rouse-Zimm modes contributions to ultrasound attenuation in polymeric mixtures [42], as well as a stretched exponential expression in the form $\alpha/f^2=A/[1+(f/f_r)]^{2(1-\beta)}+B_\infty$.

As a general result, we found that the overall experimen-

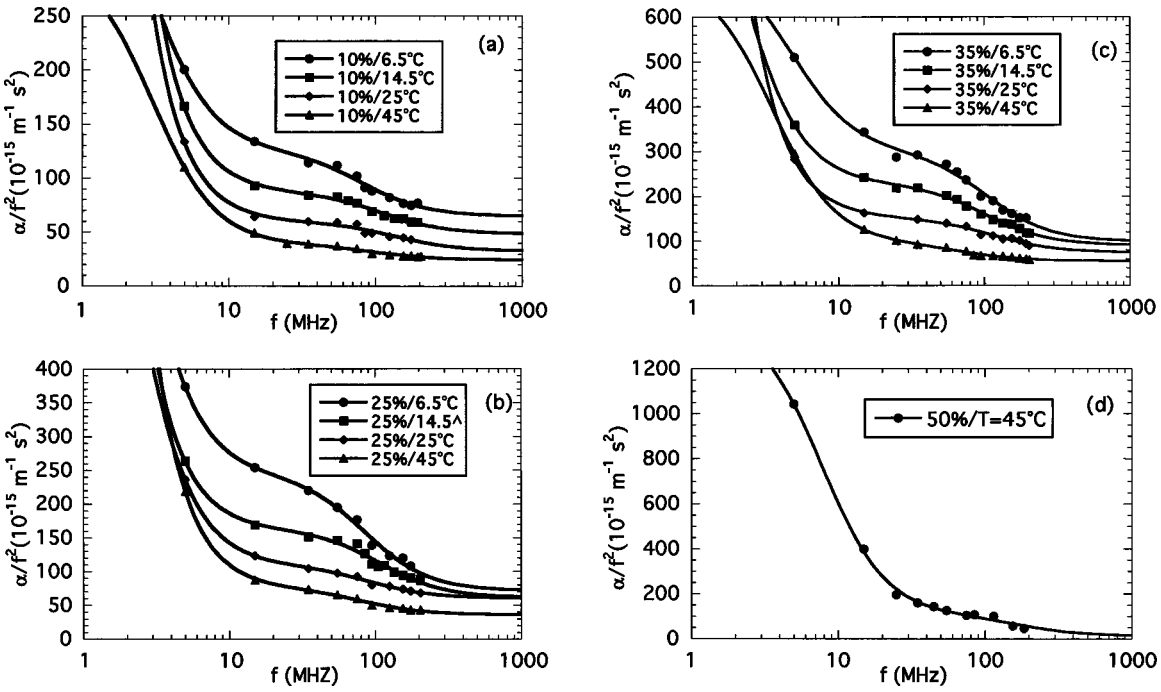

FIG. 9. Ultrasonic attenuation spectra at various concentration and temperature: (a) 10 wt %, (b) 25 wt %, (c) 35 wt %, and (d) 50 wt %. Lines through the points are two relaxation times fitting curves, as explained in the text. Most of the solutions exhibit a viscoelastic behavior, since the experimental attenuation is lower than the Navier-Stokes contribution due to the steady shear viscosity.

tal spectra could not be fitted by Eq. (12) alone, whatever $F(f^*)$. Rather, they could be well fitted by a sum of two terms $F_1(f_1^*)$ and $F_h(f_h^*)$. This finding can also be shown by a visual inspection of the spectra in the figures which show two distinct relaxation regions, the former at frequency below about 5 MHz and the latter at higher frequencies. Taking into account the lack of experimental data at very low frequency that limits the reliability of $F_1(f_1^*)$, we fit the data to the expression $\alpha/f^2 = A_1/[1+(f/f_1)^2] + F_h(f_h^*) + B_\infty$, i.e., we approximate the low f data by a single relaxation. Concerning the high frequency relaxation $F_h(f_h^*)$, we find that a Debye equation in the form $A_h/[1+(f/f_h)^2]$ well represents the data, with an accuracy comparable to that obtained from fits with continuous distributions. Thus the full spectra are approximately described by a two-relaxation-time equation. The relative fitting curves are shown in Figs. 9. The accuracy of the fitting parameters A_1 and f_1 is, of course, very poor. In contrast, the parameters (A_h, f_h) of the high frequency process are well defined, and are reported in Table I together with the background attenuation B_∞. For comparison, we also show in the table the sound attenuation in the solvent and the Navier-Stokes contribution $(\alpha/f^2)_{\mathrm{NS}}$ from the solutions. The relevant finding in the table is that most solutions exhibit a viscoelastic behaviors, since the asymptotic attenuation B_∞ is lower than $(\alpha/f^2)_{\mathrm{NS}}$.

Our absorption results give direct evidence of a viscoelastic behavior in most concentrated $C_{12}E_6$ binary mixtures. We emphasize this aspect, since most literature reports claim a viscoelastic behavior solely from an observation of sound velocity changes as a function of frequency. However, such conclusions are unacceptable or incomplete, since a sound velocity dispersion can derive from the relaxational behavior of the bulk viscosity alone.

From our experiments it is impossible to disentangle the contributions from bulk and shear viscosity. This requires independent dynamic shear viscosity $\eta(\omega)$ measurements. Also, it is difficult to assign the observed high frequency relaxation $A_h(\omega)$ to a peculiar bulk or/and shear mechanism. This process which is characterized by low amplitudes A_h and by relaxation frequencies f_h around 100 MHz (see Table I) can, in principle, be caused by several mechanisms. A chemical relaxation related to the water exchange from the bulk to the EO (oxyethylene) groups of the surfactant, or a rapid internal motion (rotational isomerism [40]) of a part of

TABLE I. Significant parameters in the attenuation α/f^2 data (in 10^{-15} m^{-1} s^2).

		10 w%						25 w%						35 w%						
T (°C)	(α/f^2) water	c m/s	η/ρ (c St)	(α/f^2) shear	B_∞	A_h	f_h (MHz)	c m/s	η/ρ (c St)	(α/f^2) shear	B_∞	A_h	f_h (MHz)	c m/s	η/ρ (c St)	(α/f^2) shear	B_∞	A_h	f_h (MHz)
6.5	43	1454	2.6	22.2	65	59.9	82.5	1490	21.2	169	71.5	171	85	1518	298.7	2247	98.2	202	105
14.5	31	1479	2.7	22.1	48.4	38.2	112.4	1501	57.8	450	61.4	100	109	1521	528	3950	90	136	102
25	21	1501	6.3	49	32.5	26.7	137	1511	118.8	906	60.4	48.4	91	1521	470.4	3518	73.6	77	116
45	13	1527	12.6	65.5	24.3	13.8	98.8	1515	34.7	263	35.8	38	84	1507	50.6	389.1	54.7	40	70

the surfactant skeleton, are examples of such a possibility. However, it could also be related to a high frequency contribution of the spectrum of the shear relaxation processes.

The lack of sound velocity dispersion in the range 5–45 MHz in our measurements is consistent with the existence of large dynamical processes of lower frequency. According to Kramer-Kronig relations [46], if the attenuation of the large amplitude process is almost relaxed in the ultrasonic range studied, the corresponding velocity should take an asymptotic high frequency (infinite) value and should depend negligibly on the frequency. Then one can reasonably argue that the observed velocity represents the high frequency velocity. This implies that the bulk modulus K_r and the rigidity modulus G_∞ are small compared to K_0. According to viscoelastic theories, small bulk viscosity and very long shear relaxation times should, in fact, give low relaxation moduli ($K_r = \eta_{b,0}/\tau_b$ and $G_\infty = \eta_{s,0}/\tau_s$), and then

$$c_\infty^2/c_0^2 = (K_0 + K_r + 4/3G_\infty)/K_0 = 1 + [(\eta_{b,0}/\tau_b + \eta_{s,0}/\tau_s)/K_0] \approx 1.$$

In the majority of our viscoelastic samples it is $(\alpha/f^2)_{\mathrm{NS}} > B_\infty > (\alpha/f^2)_{\mathrm{water}}$. However, in the 50-wt % sample at $T = 45\,^\circ$C (not reported in Table I) it is $B_\infty \approx (\alpha/f^2)_{\mathrm{water}}$, i.e., the high frequency sound waves ''see'' the pure solvent.

The present results are not inconsistent with the conclusions in Ref. [15], where at high temperatures and concentrations the authors suggested the formation of entangled aggregates of long and flexible rodlike micelles. In particular, the $B_\infty > (\alpha/f^2)_{\mathrm{water}}$ we found at 10, 25, and 35 wt % agree with the finding in flexible polymer solutions, where the high frequency dynamic viscosity is larger than the viscosity of a pure solvent. The exception is the 50-wt % sample at 45 °C, where $B_\infty \approx (\alpha/f^2)_{\mathrm{water}}$ indicates that new structural arrangements occur at higher concentrations.

V. DISCUSSION

From the viscosity analysis in the low (ϕ, T) region, we conjectured that this region is likely characterized by noninteracting globular micelles. This assumption is consistent with the behavior of the micellar modulus M_m'. According to the current models of micellization, a single micelle is made by a hydrophobic inner core possessing the soft structure of a liquidlike medium and by an outer hydrophilic shell made by the oxyethylene groups (OE) and possessing a hard structure likely due to the hydration water that packs the shell well, making it considerably resistant to compression. The models also predict [34] that $M_S' < M_m' < M_I'$, i.e., the elastic modulus of the surfactant in the micellar state above CMC (M_m'), is larger than in the pure liquid state (M_S') and lower than in the monomeric conditions below CMC (M_I'). Our results agree with such predictions, being $M_m' > M_S'$.

The finding that at high temperatures both diluted and concentrated solutions exhibit similar and softer elastic properties is an indication of a structural continuity of these solutions. From the viscosity analysis, we argued that on crossing the $T_{\eta-}$ line there is a smooth transition from noninteracting micelles to interacting or growing micellar structures. These structures could be built by dynamically connected aggregates of isolated micelles that eventually transform into a percolating network (due to increased attractive interaction), and/or by the growth of micelles into long aggregates. However, connected and percolating networks should exhibit solidlike behaviors i.e., higher M_m', in contrast with experiments. Then, we must conclude that in the high $\phi - T$ region the micelle grows into elongated and flexible structures possessing high compressibility. However since M_m' decreases, we must conclude that on increasing temperature such structures become longer and/or more flexible. On the other hand, we recall that the solutions in the hexagonal crystalline region H_1 are made by long ordered cylindrical structures. Then, looking at the lack of discontinuity of M_m' on crossing this region, either varying the concentration (for $T < 38\,^\circ$C) or the temperature (at 50 wt %), we must argue that the micellar morphology is quite similar in regions adjacent the phase H_1, i.e., the micellar organization inside and outside the T_{H_1} region is that of long rodlike aggregates. The softness of these structures suggests entanglements and large flexibility.

A support of this hypothesis (flexible and/or entangled polymericlike structures present in concentrated solutions) comes from a comparison with microemulsions made by reversed micelles (droplets of water—AOT surfactant in oil). We already noted that in these systems the viscosity exhibits trends similar to those in our nonionic binary solutions, with $T_{\eta+}$ lines (connecting viscosity maxima) related to a dynamic percolation line. However, concerning the elastic modulus there are some differences. In microemulsions studies [4,7] at fixed T, the excess high frequency moduli $\Delta M'$ (obtained from hypersonic velocities) scales with concentration according to a power law of type $\Delta M' = A(\phi - \phi_c)^t$, where $t = 2.5$, in agreement with dynamic percolation predictions. Likewise, $\Delta M'$ as a function of T exhibits, for each ϕ, maxima at temperatures corresponding to the percolation threshold. Looking at our results in Fig. 6(a), we can see that $\Delta M'$ has an approximate linear increase with ϕ (at least up to 50 wt %) while the temperature dependence in Fig. 6(b) shows a monotonic decrease. Since hypersonic moduli are always higher than ultrasonic ones, these different trends cannot be attributed to the different frequency range of measurements. Then the above analysis of the moduli again leads us to exclude that in our system the $T_{\eta+}$ line is related to a percolation line.

As in the case of viscosity, we are not able to assign a significance to this $T_{\eta+}$ line from the behavior of M_m' or $\Delta M'$, since they exhibit regular trends on crossing this line. However, the present results support the analogy between the conformation of concentrated solutions of nonionic surfactants and polymers in a good solvent, i.e., micelles that are long and flexible entangled rods. In particular, the $B_\infty > (\alpha/f^2)_{\mathrm{water}}$ we found at 10, 25, and 35 wt % agree with the finding in flexible polymer solutions where high frequency dynamic viscosity is larger than the viscosity of the solvent. The exception is the 50 wt % sample at 45 °C, where $B_\infty \approx (\alpha/f^2)_{\mathrm{water}}$ indicates that new structural arrangements occur at higher concentrations and temperatures.

VI. CONCLUSIONS

We have presented the results of a study of viscosity and ultrasonic propagation in aqueous solutions of the nonionic

surfactant $C_{12}E_6$. We observe a rapid increase of the static shear viscosity as the temperature and concentration of the micellar phase increase in the isotropic region of the phase diagram. Correspondingly, the sound absorption data show direct evidence of a viscoelastic behavior. These experimental behaviors are qualitatively similar to those observed in microemulsions of reversed micelles (droplets), where an increasing connectivity of droplets leading to a percolative regime has been invoked. However, attempts to explain our results in a consistent way on such grounds fail. In particular, we find that, on increasing concentration and temperature, the real longitudinal modulus of the surfactant phase exhibits a regular trend, in contrast to the scaled behavior found in microemulsions. In addition, we find that, as the temperature increases, the surfactant phase becomes softer and softer, i.e., it contrasts with a percolation picture where a transition toward harder solidlike structures are predicted. These findings and other aspects emerging from our analysis suggest that, in contrast to microemulsions, the concentrated nonionic binary solutions are characterized by long cylindrical micellar structures that are softer than the globular isolated micelles envisaged at low T and ϕ. Since these structures become softer and softer, it is likely that on increasing the temperature they transform into more flexible structures, e.g., entangled polymeric solutions. Then, the two $T_{\eta-}$ and $T_{\eta+}$ lines shown in Fig. 1, and characterizing the viscosity behavior of solutions, might roughly delimit regions with different micellar morphology and consequent elastic properties. From our studies, we find that the structural changes on crossing these lines in the isotropic region are rather smooth.

ACKNOWLEDGMENTS

The financial support of the Gruppo Nazionale di Struttura della Materia (GNSM) del Consiglio Nazionale delle Ricerche, Italy, and of the Istituto Nazionale di Fisica della Materia (INFM), Italy, is gratefully acknowledged. We also wish to thank Professor C. Cametti, Dr. Luca Falconi, and Dr. Arnaldo Paparelli for supplying measurements.

[1] K. F. Herzfeld and T. A. Litovitz, *Absorption and Dispersion of Ultrasonic Waves* (Academic, New York, 1959); G. Harrison, *The Dynamic Properties of Supercooled Liquids* (Academic, New York, 1976).
[2] A. J. Matheson, *Molecular Acoustics* (Wiley-Interscience, London, 1970).
[3] G. Arrigo and C. La Mesa, Phys. Rev. A **24**, 2817 (1981).
[4] L. Ye, D. A. Weitz, Ping Shen, S. Bhattacharya, J. S. Huang, and M. J. Higgins, Phys. Rev. Lett. **63**, 263 (1989); Prog. Colloid Polym. Sci. **81**, 70 (1990); L. Ye, J. Liu, P. Sheng, J. S. Huang, and D. A. Weitz, J. Phys. (Paris) Colloq. **3**, 183 (1993).
[5] C. Cametti, P. Codastefano, G. D'Arrigo, P. Tartaglia, J. Rouch, and S. H. Chen, Phys. Rev. A **42**, 3421 (1990).
[6] A. D'Aprano, G. D'Arrigo, M. Goffredi, A. Paparelli, and V. Turco Liveri, J. Chem. Phys. **95**, 1304 (1991); J. Phys. Chem. **97**, 3615 (1993).
[7] F. Mallamace, N. Micali, C. Vasi, and G. D'Arrigo, Phys. Rev. A **43**, 5710 (1991).
[8] F. Mallamace, D. Lombardo, N. Micali, S. Trusso, and C. Vasi, Phys. Rev. E **51**, 2341 (1995).
[9] V. Degiorgio, in *Physics of Amphiphiles, Micelles, Vesicles and Microemulsions*, edited by V. Degiorgio and M. Corti (North-Holland, Amsterdam, 1985), and references therein.
[10] E. Alami, N. Kamenka, A. Raharimihamina, and R. Zana, J. Colloid Interface Sci. **158**, 342 (1993).
[11] D. J. Mitchell, G. J. T. Tiddy, L. Waring, T. Bostock, and M. P. McDonald, J. Chem. Soc., Faraday Trans. 1 **79**, 975 (1983).
[12] P. G. Neeson, B. R. Jennings, and G. J. T. Tiddy, Chem. Phys. Lett. **95**, 533 (1983).
[13] R. Strey, Ber. Bunsenges. Phys. Chem. **100**, 182 (1996).
[14] See, for example, B. Lindman and H. Wennerström, J. Phys. Chem. **95**, 6053 (1991); L. J. Magid, R. Triolo, E. Caponnetti, and J. S. Johnson, Jr., in *Surfactants in Solution*, edited by K. L. Mittal and P. Bothorel (Plenum, New York, 1986), Vol. 4, p. 165.
[15] T. Kato, S. Anzai, and T. Seimiya, J. Phys. Chem. **94**, 7255 (1990).
[16] W. H. Richtering, W. Burchard, E. Jahns, and H. Finkelmann, J. Phys. Chem. **92**, 6032 (1988).
[17] S. Puvvada and D. Blanckschtein, J. Chem. Phys. **92**, 3710 (1990).
[18] See, for example, G. J. Vroege and H. N. V. Lekkerkerker, Rep. Prog. Phys. **55**, 124 (1992).
[19] R. R. Balmbra, J. S. Clunie, J. M. Corkill, and J. F. Goodman, J. Chem. Soc., Faraday Trans. **58**, 1661 (1962).
[20] M. Corti and V. Degiorgio, J. Phys. Chem. **85**, 1442 (1981).
[21] T. Kato and T. Seimiya, J. Phys. Chem. **90**, 3159 (1986).
[22] G. D'Arrigo and A. Paparelli, J. Chem. Phys. **88**, 405 (1988).
[23] R. F. Berg, M. R. Moldover, and J. S. Huang, J. Chem. Phys. **87**, 3687 (1987).
[24] M. Zulauf, in *Physics of Amphiphiles, Micelles, Vesicles and Microemulsions* (Ref. [9]), p. 663.
[25] D. Majolino, F. Venuto, and N. Micali, Phys. Rev. A **42**, 7330 (1990).
[26] S. H. Chen, F. Mallamace, J. Rouch, and P. Tartaglia, in *Slow Dynamics in Condensed Matter*, edited by K. Kawasaki, T. Kawakatsu, and M. Tokuyama (AIP, New York, 1992). Vol. 256, p. 301.
[27] M. A. van Dijk, Phys. Rev. Lett. **55**, 1003 (1985); P. Mills, J. Phys. (France) Lett. **46**, L301 (1985); J. Peyrelasse, M. Moha-Ouchane, and C. Bined, Phys. Rev. A **38**, 4155 (1988).
[28] R. C. Ball and P. Richmond, Phys. Chem. Liq. **9**, 99 (1980).
[29] V. A. Del Grosso and C. W. Mader, J. Acoust. Soc. Am. **52**, 1442 (1972).
[30] O. Nomoto and H. Endo, Bull. Chem. Soc. Jpn. **43**, 3722 (1970).
[31] G. C. Benson and O. Kiyohara, J. Chem. Thermodyn. **11**, 1061 (1979).
[32] G. Briganti and G. D'Arrigo, Prog. Colloid Polym. Sci. **105**, 272 (1997).
[33] G. D'Arrigo and A. Paparelli, Phys. Rev. E **50**, 4817 (1994).

[34] S. Harada and T. Nakagawa, J. Solution Chem. **8**, 267 (1979).
[35] P. D. Edmonds and J. Dyro, in *Reports of the Sixth International Congress on Acoustics*, edited by Dr. Y. Kahasi (Acoustic Society of Japan, Tokyo, 1968), Vol. 5, paper J-5-7.
[36] G. J. T. Tiddy, M. F. Walsh, and E. Wyn-Jones, J. Chem. Soc. Chem. Commun. **6**, 252 (1979).
[37] G. J. T. Tiddy, M. F. Walsh, and E. Wyn-Jones, J. Chem. Soc., Faraday Trans. 1 **78**, 389 (1982).
[38] K. Muralidhar, M. L. S. Swamy, S. N. Rao, and K. S. Rao, Phys. Rev. A **33**, 3477 (1986).
[39] A. Borthakur and R. Zana, J. Phys. Chem. **91**, 5957 (1987).
[40] D. B. Fenner, Phys. Lett. **94A**, 444 (1983); J. Chem. Phys. **81**, 5179 (1984).
[41] Y. Harada and M. Tabuchi, in *Slow Dynamics in Condensed Matter* (Ref. [26]), p. 320.
[42] W. Mayer, S. Hoffmann, G. Meier, and I. Alig, Phys. Rev. E **55**, 3102 (1997).
[43] See, for example, M. Findi, B. Michels, and R. Zana, J. Phys. Chem. **96**, 6095 (1992); S. Kato, S. Harada, and H. Sahara, *ibid.* **99**, 12 570 (1995).
[44] E. A. G. Aniansson and S. Wall, J. Chem. Phys. **78**, 1024 (1974); **79**, 857 (1975).
[45] M. Teubner, J. Chem. Phys. **83**, 2917 (1979).
[46] M. O'Donnell, E. T. Jaines, and J. Miller, J. Acoust. Soc. Am. **69**, 696 (1981).